Acta Cryst E CRYSTALLOGRAPHIC COMMUNICATIONS

ISSN 2056-9890

Synthesis, structure and energy calculations of 4-{4-[(2,3-dioxoindol-1-yl)methyl]-1*H*-1,2,3-triazol-1-yl}butyl acetate

Sanaa Sabir,[a] Nour El Hoda Mustaphi,[a]* Daouda Ballo,[b] Olivier Blacque,[c] Tuncer Hökelek[d] and Nada Kheira Sebbar[a]

[a]Laboratory of Heterocyclic Organic Chemistry, Medicines Science Research Center, Pharmacochemistry Competence Center, Mohammed V University in Rabat, Faculty of Sciences, Av. Ibn Battouta, BP 1014, Rabat, Morocco, [b]Laboratory of Constitution and Reaction of Matter (LCRM), UFR SSMT, Félix Houphouët Boigny University, 22 B.P. 582 Abidjan 22, Republic of Côte d'Ivoire, [c]University of Zurich, Department of Chemistry B, Winterthurerstrasse 190, 8057 Zurich, Switzerland, and [d]Department of Physics, Hacettepe University, 06800 Beytepe, Ankara, Türkiye. *Correspondence e-mail: nourelhoda.mustaphi@fsr.um5.ac.ma

Received 12 May 2026
Accepted 4 July 2026

Edited by D. R. Manke, University of Massachusetts Dartmouth, USA

Keywords: crystal structure; hydrogen bond; π-stacking; isatin.

CCDC reference: 2570724

Supporting information: this article has supporting information at journals.iucr.org/e

The title compound, $C_{17}H_{18}N_4O_4$, consists of almost planar isatin and triazole rings inclined by 78.47 (5)°, as well as a butyl acetate moiety bonded to the N atom of the triazole ring. In the crystal, molecules link into a semicolon shape along the *b*-axis direction through bifurcated C—H···O hydrogen bonds. Aromatic π–π and C—H···π(ring) interactions also help to consolidate the crystal packing. The Hirshfeld surface analysis of the crystal structure indicates that the most important contributions for the crystal packing are from H···H (40.6%), H···O/O···H (26.6%), H···N/N···H (13.8%) and H···C/C···H (8.9%) interactions. The volume of the crystal voids and the percentage of free space in the unit cell were calculated to be 82.1 Å^3 and 10.0%, respectively, showing that there is no large cavity in the crystal packing. Computational methods revealed C—H···O hydrogen-bonding energy of −11.6 kJ mol^{-1}. The evaluation of the electrostatic, dispersion and total energy frameworks indicates that the stabilization is dominated *via* the dispersion energy contributions in the crystal structure.

1. Chemical context

Isatins and their derivatives are versatile intermediates in organic synthesis owing to their structural diversity. In addition, they have attracted considerable attention because of the broad range of pharmacological activities exhibited by many of their derivatives (Melis *et al.*, 2017). These compounds are associated with a wide range of biological activities, including antibacterial, antifungal, antiviral, antimicrobial, anticancer, anti-inflammatory, anticonvulsant, anti-COVID and anti-tuberculosis activities (Song *et al.*, 2020; Feng *et al.*, 2010; Ghafil *et al.*, 2019; Shagufta & Ahmad, 2021; Gowrivel Vijayakumar *et al.*, 2023; Obafemi *et al.*, 2021; Rasgania *et al.*, 2023). Furthermore, nitrogen heterocycles, particularly the 1,2,3-triazole motif, are attracting increasing interest due to their medicinal properties. In this context, our laboratory has conducted several studies on the functionalization of the triazole nucleus and its integration with various heterocyclic systems (El Atrassi *et al.*, 2024; Zouhair *et al.*, 2023). Continuing our research on copper-catalyzed azide–alkyne cycloaddition reactions using click chemistry, we present herein the molecular and crystal structures, Hirshfeld surface analysis and intermolecular interaction energy calculations of the title compound, 4-{4-[(2,3-dioxoindol-1-yl)methyl]-1*H*-1,2,3-triazol-1-yl}butyl acetate, **3**. It was obtained by treating 1-(prop-2-

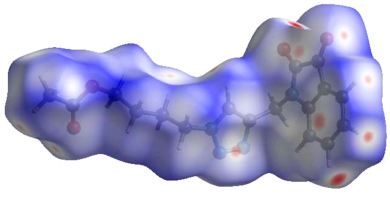

ynyl)isatin, **1**. with 4-azidobutyl acetate, **2**, in the presence of copper sulfate and sodium ascorbate as reducing agents, in a 1:1 water/ethanol mixture. After stirring for 20 h at room temperature, the reaction selectively leads to the 1,4-disubstituted triazole regioisomer (Scheme 1).

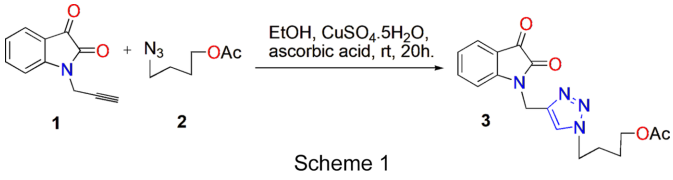

Scheme 1

2. Structural commentary

The title compound consists of methylene-bridged triazole and isatin rings, and a butyl acetate moiety bonded to the N atom of the triazole ring (Fig. 1). The almost planar isatin *A* (C1–C6) and *B* (N1/C1/C6–C8) rings are oriented at a dihedral angle of 1.13 (5)°, where atoms O1 and O2 are 0.0229 (12) and −0.0687 (13) Å away from the best plane of ring *B*, respectively. Thus, they are almost coplanar with the corresponding ring plane. The almost planar isatin ring is inclined to the triazole ring, *C* (C10/C11/N2–N4), by 78.47 (5)°. Atoms C9 and C12 are 0.0007 (16) and −0.0022 (18) Å away from the best plane of ring *C*.

3. Supramolecular features

In the crystal, the molecules link into a semicolon shape along the *b*-axis direction through bifurcated C—H···O hydrogen bonds (Table 1 and Fig. 2). Aromatic π–π interactions with centroid-to-centroid distance, dihedral angle and slippage values of 3.6558 (10) Å, 1.13 (9)° and 1.62 Å, respectively, between isatin rings *A* and *B*, and C—H···π(ring) interactions (Table 1) also help to consolidate the crystal packing.

Table 1
Hydrogen-bond geometry (Å, °).

*Cg*2 is the centroid of the N2–N4/C10/C11 ring.

D—H···*A*	*D*—H	H···*A*	*D*···*A*	*D*—H···*A*
C3—H3···O2^{i}	0.95	2.50	3.291 (2)	141
C9—H9*B*···*Cg*2^{ii}	0.99	2.67	3.6005 (17)	162

Symmetry codes: (i) $x-1, y+1, z$; (ii) $x+1, y, z$.

4. Database survey

A search of the Cambridge Structural Database (CSD; Groom *et al.*, 2016; updated to May 2026) using the search fragment isatin (see Scheme 2) revealed several structures closely related to the title compound, all containing an isatin (indoline-2,3-dione) core substituted at the N1 position with different alkyl or heterocyclic substituents (see Scheme 2). Among these, compound **I** (CSD entry 717335, refcode KOMREK; Ji *et al.*, 2009), with *R*1 = C_4H_9, *R*2 = Br and *R*3 = H, represents a 5-bromo-substituted isatin derivative bearing a linear N-alkyl chain. Such derivatives are commonly reported in the literature and generally show a planar indoline-2,3-dione framework, with the N-alkyl substituent adopting an extended conformation to reduce steric interactions. Compound **II** (CSD entry 858493, refcode OCAYOI; Liu *et al.*, 2011) is characterized by *R*1 = $C_6H_{13}NO$, *R*2 = H and *R*3 = H, and contains a heterocyclic morpholine moiety attached through an alkyl linker to the isatin N atom. Similar morpholine-containing derivatives are known to promote additional intermolecular contacts through weak C—H···O interactions, particularly involving the O atoms of the morpholine ring. In compound **III** (CSD entry 786667, refcode YUPSUY; Tang *et al.*, 2010), with *R*1 = CH_2–C_6H_5, *R*2 = Cl and *R*3 = H, the isatin ring is substituted by a chloro group on the aromatic ring and connected to a benzyl fragment through the N atom. The presence of the aromatic substituent favours π–π stacking interactions, which may contribute significantly to the stabilization of the crystal packing, while compound **IV** (CSD entry 1437567, refcode OXIMEP; Bogdanov *et al.*, 2016), with *R*1 = $C_{15}H_{22}N_2$, *R*2 = H and *R*3 = Br, exhibits a more extended structure, incorporating both a bromo-substi-

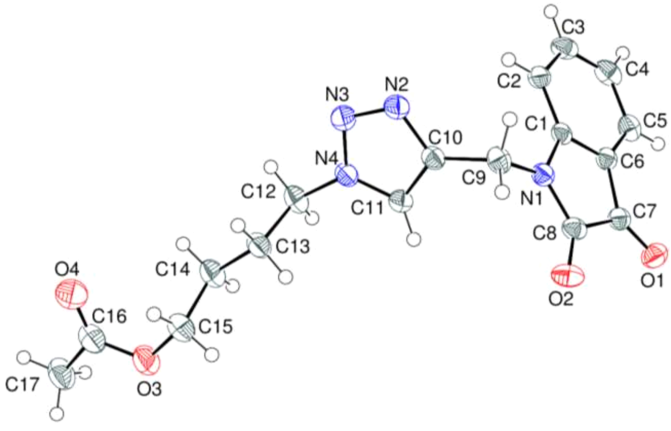

Figure 1
The title molecule with the atom-labelling scheme and 50% probability ellipsoids.

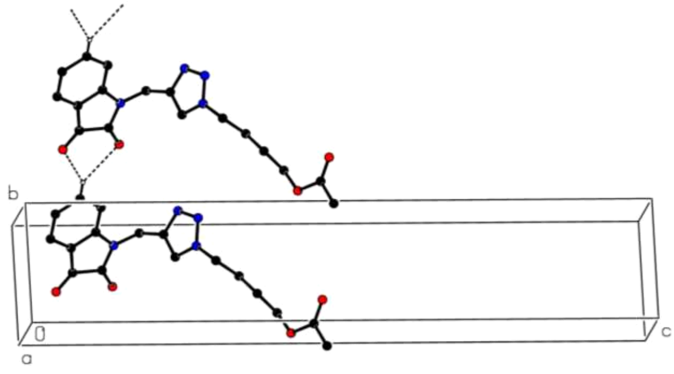

Figure 2
Packing viewed along the *a*-axis direction with C—H···O hydrogen bonds depicted by dashed lines.

tuted isatin unit and a piperazine-based linker connected to an aryl fragment. Such flexible linkers often facilitate conformational adaptability and allow the formation of multiple weak intermolecular interactions, including C—H···O hydrogen bonds and aromatic interactions. These structural similarities support the relevance of previously reported isatin derivatives as reference systems and provide useful insight into the expected conformational behaviour and intermolecular interactions in the crystal structure of the title compound.

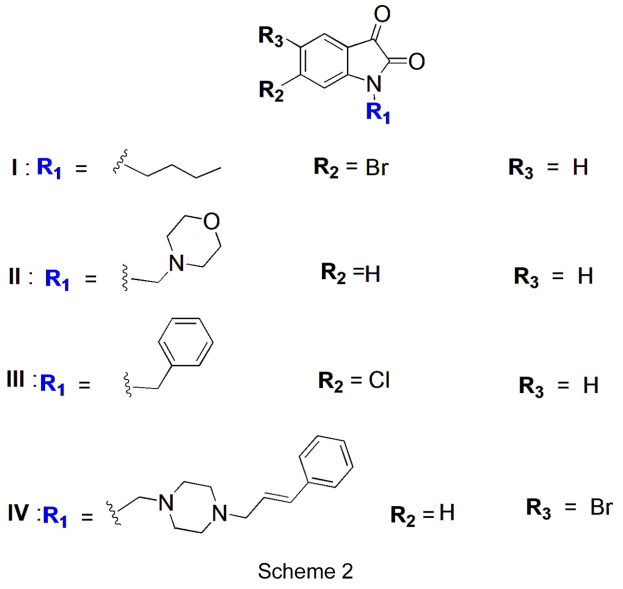

Scheme 2

5. Hirshfeld surface analysis

The intermolecular interactions in the crystal were visualized by carrying out Hirshfeld surface (HS) analysis using *CrystalExplorer* (Version 17.5; Spackman *et al.*, 2021). Fig. 3 shows the Hirshfeld surface in the crystal. The white surface indicates contacts with distances equal to the sum of the van der Waals radii and the red and blue colours indicate distances shorter (in close contact) or longer (distinct contacts) than the van der Waals radii, respectively. The red spots indicate their roles as the respective donor and/or acceptor atoms; they also appear as the blue and red regions corresponding to positive and

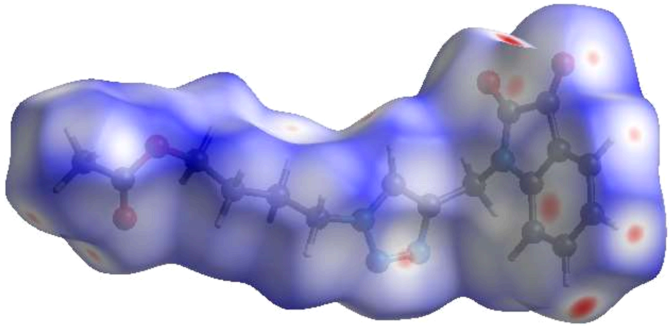

Figure 3
View of the three-dimensional Hirshfeld surface of the title compound plotted over d_{norm} in the range from −0.17 to 1.29 a.u.

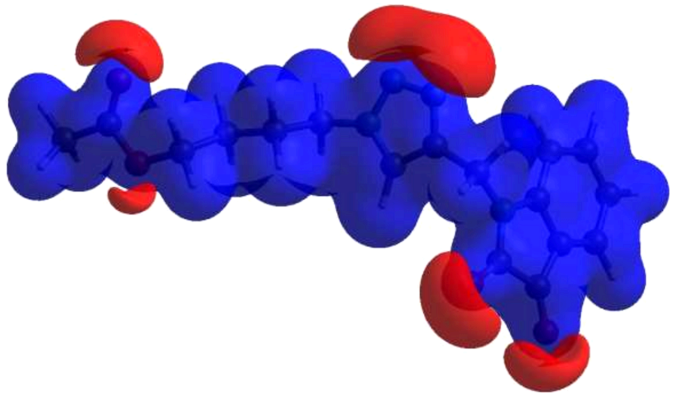

Figure 4
View of the three-dimensional Hirshfeld surface of the title compound plotted over electrostatic potential in the range from −0.05 to 0.05 a.u. using the STO-3 G basis set at the Hartree–Fock level of theory. Hydrogen-bond donors and acceptors are shown as blue and red regions around the atoms, corresponding to positive and negative potentials, respectively.

negative potentials on the HS mapped over electrostatic potential as shown in Fig. 4. The blue and red regions indicate positive (hydrogen-bond donors) and negative (hydrogen-bond acceptors) electrostatic potentials. The overall two-dimensional fingerprint plot is shown in Fig. 5(*a*) and those delineated into various contact types are illustrated in Figs. 5(*b*)–(*j*). According to the fingerprint plots, H···H, H···O/O···H, H···N/N···H and H···C/C···H contacts make the most significant contributions to the HS, at 40.6, 26.6, 13.8 and 8.9%, respectively (Fig. 5).

The strength of the crystal packing depends on the tight packing of the molecules, which results in insignificant voids. The volume of the crystal voids [Figs. 6(*a*) and 6(*b*)] and the percentage of free space in the unit cell were calculated as 82.11 Å^3 and 9.96%, respectively.

6. Interaction energy calculations and energy frameworks

The intermolecular interaction energies were calculated using CE-B3LYP/6-31G(d,p) energy model available in *CrystalExplorer* (Version 17.5; Spackman *et al.*, 2021), where a cluster of molecules is generated by applying crystallographic symmetry operations with respect to a selected central molecule within the radius of 3.8 Å by default. Hydrogen-bonding interaction energies (in kJ mol^{-1}) were calculated to be −4.9 (E_{ele}), −0.7 (E_{pol}), −11.3 (E_{dis}), 5.0 (E_{rep}) and −11.6 (E_{tot}) for C3—H3···O2 hydrogen-bonding interactions.

Energy frameworks combine the calculation of intermolecular interaction energies with a graphical representation of their magnitude, in which they were constructed for E_{ele} (red cylinders), E_{dis} (green cylinders) and E_{tot} (blue cylinders) [Figs. 7(*a*), 7(*b*) and 7(*c*)]. The evaluation of the electrostatic, dispersion and total energy frameworks indicates that the stabilization is dominated *via* the dispersion energy contributions in the crystal structure of the title compound.

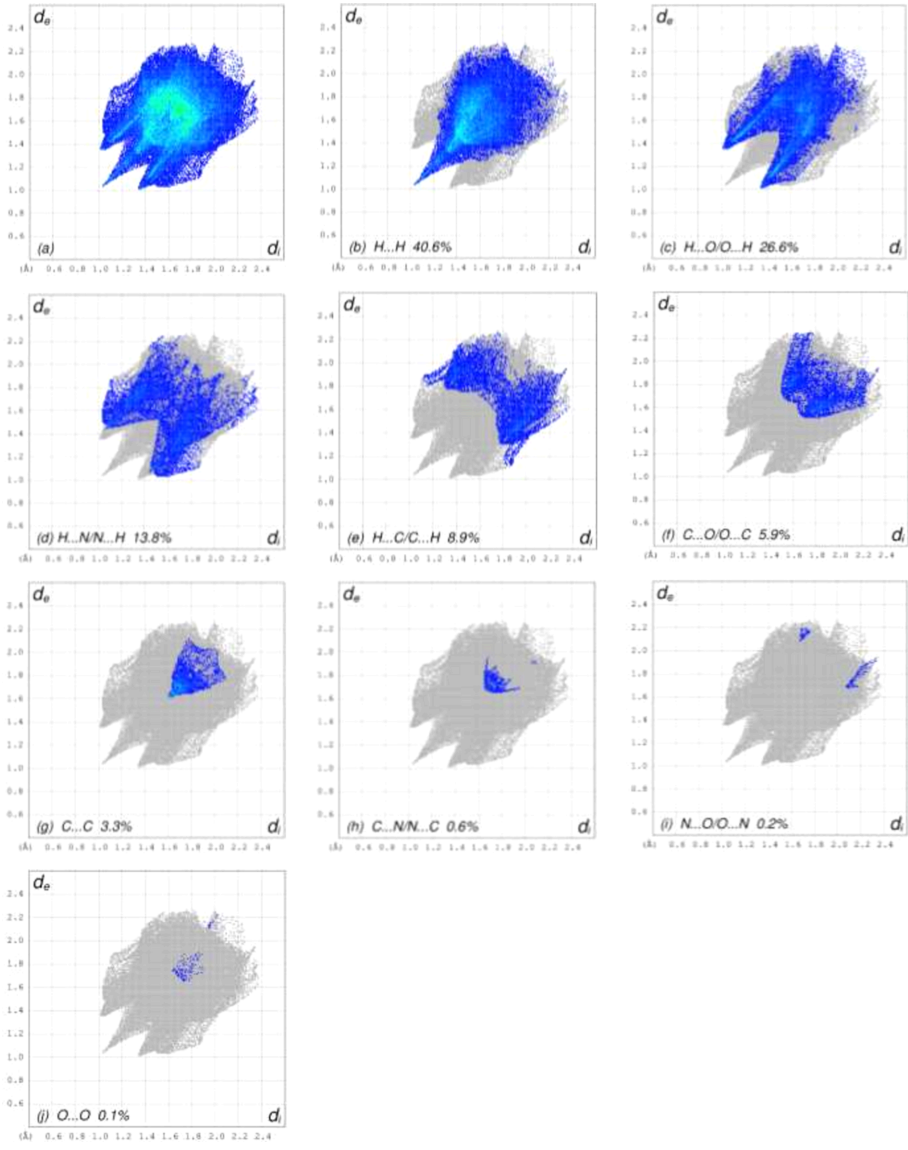

Figure 5
The two-dimensional fingerprint plots of the title compound, showing (*a*) all interactions, and delineated into (*b*) H···H, (*c*) H···O/O···H, (*d*) H···N/N···H, (*e*) H···C/C···H, (*f*) C···O/O···C, (*g*) C···C, (*h*) C···N/N···C, (*i*) N···O/O···N and (*j*) O···O interactions. The d_i and d_e values are the closest internal and external distances (in Å) from given points on the Hirshfeld surface contacts.

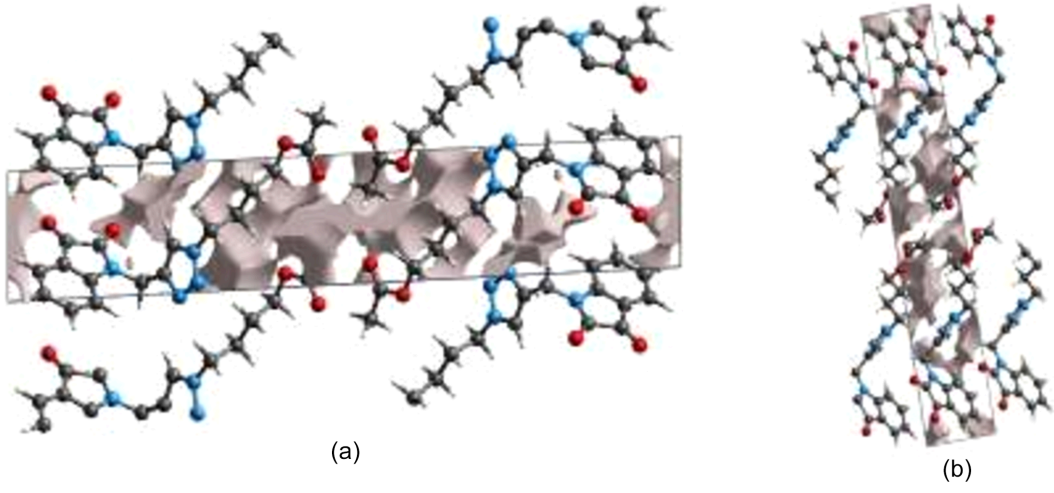

Figure 6
Graphical view of voids in the crystal (*a*) along the *a*-axis direction and (*b*) along the *b*-axis direction.

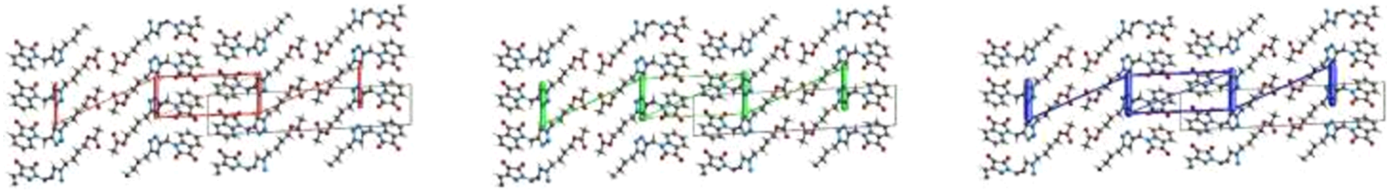

Figure 7
The energy frameworks for a cluster of molecules of the title compound viewed down the *a* axis, showing the (*a*) electrostatic energy, (*b*) dispersion energy and (*c*) total energy diagrams. The cylindrical radius is proportional to the relative strength of the corresponding energies and they were adjusted to the same scale factor of 80 with a cut-off value of 5 kJ mol^{-1} within 2 × 2 × 2 unit cells.

7. Synthesis and crystallization

1-(Prop-2-ynyl)isatin, **1** (2.7 mmol), and 4-azidobutyl acetate, **2** (2.7 mmol), were dissolved in 10 ml of ethanol. To this solution, $CuSO_4{\cdot}5H_2O$ (1.62 mmol) and sodium ascorbate (2.7 mmol), previously dissolved in 10 ml of distilled water, were added. The reaction mixture was stirred at room temperature for 20 h. After completion of the reaction, the mixture was filtered and the solvent was removed under reduced pressure. The obtained residue was purified by column chromatography on silica gel using an ethyl acetate/hexane (8:2 *v*/*v*) mixture as the eluent. The resulting solid was filtered, washed with water, dried and recrystallized from ethanol solution to afford the title compound **3** in 85% yield.

^{1}H NMR (500 MHz, DMSO-d_6): δ (ppm) 8.13 (*s*, 1H, –$CH_{triazole}$), 7.60–7.07 (*m*, 4H, CH_{ar}), 4.91 (*s*, 2H, NCH_2), 4.29 (*t*, 2H, OCH_2), 3.92 (*t*, 2H, NCH_2), 1.93 (*s*, 3H, CH_3), 1.42–1.80 (*m*, 4H, –CH_2–CH_2–). ^{13}C NMR (125 MHz, DMSO-d_6): δ (ppm) 183.65, 170.93 (C═O); 158.33, 150.69, 138.60 (Cq); 124.16 (–$CH_{triazole}$), 125.00, 123.89, 118.13, 111.70 (CH_{ar}), 63.63, 49.53, 35.60, 26.82, 25.63 (CH_2), 21.21 (CH_3).

8. Refinement

Crystal data, data collection and structure refinement details are summarized in Table 2. C-bound H atoms were positioned geometrically (C—H = 0.95–0.99 Å). All were included as riding contributions with isotropic displacement parameters 1.2–1.5 times those of the attached atoms.

Acknowledgements

TH is grateful to Hacettepe University Scientific Research Project Unit (grant No. 013 D04 602 004).

References

Bogdanov, A. V., Vazykhova, A. M., Khasiyatullina, N. R., Krivolapov, D. B., Dobrynin, A. B., Voloshina, A. D. & Mironov, V. F. (2016). *Khim. Geterotsikl. Soedin.* **52**, 25

Clark, R. C. & Reid, J. S. (1995). *Acta Cryst.* A**51**, 887–897.

Dolomanov, O. V., Bourhis, L. J., Gildea, R. J., Howard, J. A. K. & Puschmann, H. (2009). *J. Appl. Cryst.* **42**, 339–341.

El Atrassi, Z., Benzekri, Z., Blacque, O., Hökelek, T., Mazzah, A., Cherkaoui, H. & Sebbar, N. K. (2024). *J. Mol. Struct.* **80**, 1075–1080.

Feng, L. S., Liu, M. L., Wang, B., Chai, Y., Hao, X. Q., Meng, S. & Guo, H. Y. (2010). *Eur. J. Med. Chem.* **45**, 3407–3412.

Ghafil, R. A. A., Obaid, N. H. & Aljamali, N. M. (2019). *J. Adv. Res. Dyn. Control Syst.* **11**, 199–209.

Gowrivel Vijayakumar, B., Ramesh, D., Kumari, S., Maity, A., Pinnaka, A. K. & Kannan, T. (2023). *Int. J. Biol. Macromol.* **244**, 125428.

Groom, C. R., Bruno, I. J., Lightfoot, M. P. & Ward, S. C. (2016). *Acta Cryst.* B**72**, 171–179.

Ji, L., Fang, Q. & Fan, J. (2009). *Acta Cryst.* E**65**, o136.

Liu, H., Fan, D., Wang, D. & Ou-yang, P.-K. (2011). *Acta Cryst.* E**67**, o3427.

Melis, C., Meleddu, R., Angeli, A., Distinto, S., Bianco, G., Capasso, C., Cottiglia, F., Angius, R., Supuran, C. T. & Maccioni, E. (2017). *J. Enzyme Inhib. Med. Chem.* **32**, 68–73.

Obafemi, C. A., Adegbite, O. B., Fadare, O. A., Iwalewa, E. O., Omisore, N. O., Sanusi, K., Yilmaz, Y. & Ceylan, U. (2021). *Heliyon* **7**, e05756.

Table 2
Experimental details.

Crystal data	
Chemical formula	$C_{17}H_{18}N_4O_4$
M_r	342.35
Crystal system, space group	Triclinic, $P\overline{1}$
Temperature (K)	160
a, *b*, *c* (Å)	4.9945 (3), 5.6496 (2), 29.7750 (8)
α, β, γ (°)	92.618 (3), 91.094 (3), 100.609 (4)
V (Å^3)	824.61 (6)
Z	2
Radiation type	Cu *K*α
μ (mm^{-1})	0.84
Crystal size (mm)	0.22 × 0.10 × 0.02
Data collection	
Diffractometer	Agilent SuperNova Dual Source diffractometer with an Atlas detector
Absorption correction	Analytical [*CrysAlis PRO* (Rigaku OD, 2023) based on expressions derived by Clark & Reid (1995)]
T_{min}, T_{max}	0.882, 0.981
No. of measured, independent and observed [$I > 2\sigma(I)$] reflections	17659, 3459, 3103
R_{int}	0.028
(sin $\theta/\lambda)_{max}$ (Å^{-1})	0.631
Refinement	
$R[F^2 > 2\sigma(F^2)]$, $wR(F^2)$, *S*	0.049, 0.136, 1.04
No. of reflections	3459
No. of parameters	227
H-atom treatment	H-atom parameters constrained
$\Delta\rho_{max}$, $\Delta\rho_{min}$ (e Å^{-3})	0.51, −0.27

Computer programs: *CrysAlis PRO* (Rigaku OD, 2023), *SHELXT* (Sheldrick, 2015*a*), *SHELXL* (Sheldrick, 2015*b*) and *OLEX2* (Dolomanov *et al.*, 2009).

Rasgania, J., Gavadia, R., Nimesh, S., Loveleen, L., Mor, S., Singh, D. & Jakhar, K. (2023). *J. Mol. Struct.* **1294**, 136464.
Rigaku OD (2023). *CrysAlis PRO*. Rigaku Oxford Diffraction Ltd, Yarnton, England.
Shagufta & Ahmad, I. (2021). *Eur. J. Med. Chem.* **213**, 113157.
Sheldrick, G. M. (2015*a*). *Acta Cryst.* A**71**, 3–8.
Sheldrick, G. M. (2015*b*). *Acta Cryst.* C**71**, 3–8.
Song, F., Li, Z., Bian, Y., Huo, X., Fang, J., Shao, L. & Zhou, M. (2020). *Arch. Pharm.* **353**, 2000143.
Spackman, P. R., Turner, M. J., McKinnon, J. J., Wolff, S. K., Grimwood, D. J., Jayatilaka, D. & Spackman, M. A. (2021). *J. Appl. Cryst.* **54**, 1006–1011.
Tang, Y., Zhang, J., Miao, Y. & Chen, G. (2010). *Acta Cryst.* E**66**, o1748.
Zouhair, M., El Ghayati, L., El Monfalouti, H., Abchihi, H., Hökelek, T., Ahmed, M., Mague, J. T. & Sebbar, N. K. (2023). *Acta Cryst.* E**79**, 1179–1182.

supporting information

Acta Cryst. (2026). E**82**, 913-918 [https://doi.org/10.1107/S2056989026006985]

Synthesis, structure and energy calculations of 4-{4-[(2,3-dioxoindol-1-yl)methyl]-1*H*-1,2,3-triazol-1-yl}butyl acetate

Sanaa Sabir, Nour El Hoda Mustaphi, Daouda Ballo, Olivier Blacque, Tuncer Hökelek and Nada Kheira Sebbar

Computing details

4-{4-[(2,3-Dioxoindolin-1-yl)methyl]-1*H*-1,2,3-triazol-1-yl}butyl acetate

Crystal data

$C_{17}H_{18}N_4O_4$
M_r = 342.35
Triclinic, $P\overline{1}$
a = 4.9945 (3) Å
b = 5.6496 (2) Å
c = 29.7750 (8) Å
α = 92.618 (3)°
β = 91.094 (3)°
γ = 100.609 (4)°
V = 824.61 (6) Å^3
Z = 2
$F(000)$ = 360
D_x = 1.379 Mg m^{-3}
Cu $K\alpha$ radiation, λ = 1.54184 Å
Cell parameters from 9479 reflections
θ = 2.9–76.1°
μ = 0.84 mm^{-1}
T = 160 K
Plate, yellow
0.22 × 0.10 × 0.02 mm

Data collection

Agilent SuperNova Dual Source diffractometer with an Atlas detector
Radiation source: micro-focus sealed X-ray tube, SuperNova (Cu) X-ray Source
Mirror monochromator
Detector resolution: 10.3801 pixels mm^{-1}
ω scans
Absorption correction: analytical [CrysAlis PRO (Rigaku OD, 2023) based on expressions derived by Clark & Reid (1995)]
T_{min} = 0.882, T_{max} = 0.981
17659 measured reflections
3459 independent reflections
3103 reflections with $I > 2\sigma(I)$
R_{int} = 0.028
θ_{max} = 76.6°, θ_{min} = 3.0°
h = −6→5
k = −7→7
l = −36→37

Refinement

Refinement on F^2
Least-squares matrix: full
$R[F^2 > 2\sigma(F^2)]$ = 0.049
$wR(F^2)$ = 0.136
S = 1.04
3459 reflections
227 parameters
0 restraints
Primary atom site location: dual
Hydrogen site location: inferred from neighbouring sites
H-atom parameters constrained
$w = 1/[\sigma^2(F_o^2) + (0.0668P)^2 + 0.4801P]$ where $P = (F_o^2 + 2F_c^2)/3$
$(\Delta/\sigma)_{max} < 0.001$
$\Delta\rho_{max}$ = 0.51 e Å^{-3}
$\Delta\rho_{min}$ = −0.27 e Å^{-3}

Special details

Geometry. All esds (except the esd in the dihedral angle between two l.s. planes) are estimated using the full covariance matrix. The cell esds are taken into account individually in the estimation of esds in distances, angles and torsion angles; correlations between esds in cell parameters are only used when they are defined by crystal symmetry. An approximate (isotropic) treatment of cell esds is used for estimating esds involving l.s. planes.

Fractional atomic coordinates and isotropic or equivalent isotropic displacement parameters (Å²)

	x	*y*	*z*	U_{iso}*/U_{eq}
C1	0.5941 (3)	0.8651 (3)	0.12378 (5)	0.0244 (3)
O1	0.8299 (3)	0.4135 (2)	0.06066 (4)	0.0359 (3)
N1	0.7712 (3)	0.7873 (2)	0.15507 (4)	0.0266 (3)
N2	0.5297 (3)	1.0272 (3)	0.25532 (5)	0.0336 (3)
C2	0.4401 (3)	1.0424 (3)	0.13060 (6)	0.0297 (3)
H2	0.444897	1.131064	0.158583	0.036*
O2	1.0351 (3)	0.4925 (2)	0.15571 (5)	0.0388 (3)
O3	−0.0057 (3)	−0.1044 (3)	0.41232 (5)	0.0487 (4)
N3	0.3379 (3)	0.9303 (3)	0.28220 (5)	0.0359 (3)
C3	0.2764 (3)	1.0851 (3)	0.09418 (7)	0.0355 (4)
H3	0.166825	1.205050	0.097685	0.043*
N4	0.3123 (3)	0.6905 (2)	0.27636 (5)	0.0292 (3)
C4	0.2700 (3)	0.9576 (3)	0.05335 (7)	0.0370 (4)
H4	0.158133	0.992594	0.029307	0.044*
O4	−0.1601 (4)	0.1441 (3)	0.46164 (6)	0.0576 (4)
C5	0.4249 (3)	0.7789 (3)	0.04694 (6)	0.0321 (4)
H5	0.420168	0.690571	0.018921	0.039*
C6	0.5866 (3)	0.7334 (3)	0.08273 (5)	0.0259 (3)
C7	0.7682 (3)	0.5599 (3)	0.08716 (6)	0.0274 (3)
C8	0.8814 (3)	0.6018 (3)	0.13693 (6)	0.0285 (3)
C9	0.8482 (3)	0.9034 (3)	0.19918 (5)	0.0305 (3)
H9A	0.894921	1.079947	0.196291	0.037*
H9B	1.012978	0.848797	0.210611	0.037*
C10	0.6267 (3)	0.8493 (3)	0.23255 (5)	0.0272 (3)
C11	0.4879 (3)	0.6326 (3)	0.24582 (6)	0.0299 (3)
H11	0.510637	0.475817	0.235690	0.036*
C12	0.1137 (4)	0.5298 (3)	0.30171 (6)	0.0357 (4)
H12A	0.017137	0.397264	0.281207	0.043*
H12B	−0.023027	0.620710	0.313763	0.043*
C13	0.2465 (4)	0.4238 (3)	0.34027 (6)	0.0338 (4)
H13A	0.325917	0.554284	0.362599	0.041*
H13B	0.395924	0.346606	0.328798	0.041*
C14	0.0386 (4)	0.2376 (4)	0.36290 (7)	0.0397 (4)
H14A	−0.093743	0.319560	0.378798	0.048*
H14B	−0.062856	0.122226	0.339769	0.048*
C15	0.1796 (5)	0.1022 (4)	0.39614 (7)	0.0445 (5)
H15A	0.334513	0.046181	0.381481	0.053*
H15B	0.253196	0.212855	0.422012	0.053*
C16	−0.1647 (5)	−0.0566 (4)	0.44583 (7)	0.0449 (5)

C17	−0.3463 (5)	−0.2781 (4)	0.46057 (7)	0.0504 (5)
H17A	−0.467339	−0.351486	0.435409	0.076*
H17B	−0.455711	−0.234972	0.485580	0.076*
H17C	−0.235198	−0.393172	0.470384	0.076*

Atomic displacement parameters (Å²)

	U^{11}	U^{22}	U^{33}	U^{12}	U^{13}	U^{23}
C1	0.0194 (7)	0.0250 (7)	0.0287 (7)	0.0025 (5)	0.0044 (5)	0.0078 (6)
O1	0.0359 (6)	0.0308 (6)	0.0413 (7)	0.0074 (5)	0.0049 (5)	−0.0033 (5)
N1	0.0258 (6)	0.0281 (7)	0.0265 (7)	0.0057 (5)	0.0009 (5)	0.0049 (5)
N2	0.0420 (8)	0.0249 (7)	0.0329 (7)	0.0035 (6)	0.0040 (6)	0.0014 (5)
C2	0.0266 (8)	0.0259 (8)	0.0375 (9)	0.0050 (6)	0.0086 (6)	0.0062 (6)
O2	0.0385 (7)	0.0322 (6)	0.0483 (8)	0.0126 (5)	−0.0077 (5)	0.0066 (5)
O3	0.0645 (9)	0.0399 (8)	0.0412 (8)	0.0051 (7)	0.0104 (7)	0.0101 (6)
N3	0.0454 (9)	0.0291 (7)	0.0329 (7)	0.0055 (6)	0.0057 (6)	0.0005 (6)
C3	0.0235 (8)	0.0314 (8)	0.0543 (11)	0.0083 (6)	0.0055 (7)	0.0145 (8)
N4	0.0349 (7)	0.0266 (7)	0.0259 (6)	0.0042 (5)	0.0004 (5)	0.0046 (5)
C4	0.0247 (8)	0.0420 (10)	0.0446 (10)	0.0042 (7)	−0.0040 (7)	0.0166 (8)
O4	0.0773 (11)	0.0380 (8)	0.0574 (10)	0.0079 (7)	0.0118 (8)	0.0064 (7)
C5	0.0254 (8)	0.0383 (9)	0.0313 (8)	0.0011 (6)	−0.0005 (6)	0.0068 (7)
C6	0.0212 (7)	0.0273 (7)	0.0292 (8)	0.0031 (6)	0.0037 (6)	0.0051 (6)
C7	0.0233 (7)	0.0252 (7)	0.0332 (8)	0.0025 (6)	0.0037 (6)	0.0044 (6)
C8	0.0242 (7)	0.0243 (7)	0.0366 (9)	0.0024 (6)	0.0020 (6)	0.0062 (6)
C9	0.0300 (8)	0.0312 (8)	0.0281 (8)	−0.0003 (6)	−0.0005 (6)	0.0032 (6)
C10	0.0310 (8)	0.0255 (7)	0.0244 (7)	0.0033 (6)	−0.0018 (6)	0.0027 (6)
C11	0.0346 (8)	0.0247 (8)	0.0306 (8)	0.0051 (6)	0.0024 (6)	0.0028 (6)
C12	0.0336 (9)	0.0386 (9)	0.0337 (9)	0.0008 (7)	0.0031 (7)	0.0110 (7)
C13	0.0402 (9)	0.0303 (8)	0.0301 (8)	0.0031 (7)	0.0020 (7)	0.0073 (6)
C14	0.0418 (10)	0.0397 (10)	0.0372 (9)	0.0033 (8)	0.0056 (8)	0.0121 (8)
C15	0.0518 (11)	0.0396 (10)	0.0426 (10)	0.0068 (8)	0.0079 (9)	0.0138 (8)
C16	0.0521 (12)	0.0447 (11)	0.0377 (10)	0.0063 (9)	0.0012 (8)	0.0109 (8)
C17	0.0651 (14)	0.0415 (11)	0.0403 (11)	−0.0035 (10)	0.0062 (9)	0.0097 (8)

Geometric parameters (Å, º)

C1—N1	1.4115 (19)	C6—C7	1.461 (2)
C1—C2	1.381 (2)	C7—C8	1.568 (2)
C1—C6	1.398 (2)	C9—H9A	0.9900
O1—C7	1.202 (2)	C9—H9B	0.9900
N1—C8	1.366 (2)	C9—C10	1.500 (2)
N1—C9	1.453 (2)	C10—C11	1.370 (2)
N2—N3	1.317 (2)	C11—H11	0.9500
N2—C10	1.354 (2)	C12—H12A	0.9900
C2—H2	0.9500	C12—H12B	0.9900
C2—C3	1.402 (2)	C12—C13	1.516 (2)
O2—C8	1.213 (2)	C13—H13A	0.9900
O3—C15	1.457 (2)	C13—H13B	0.9900

O3—C16	1.335 (3)	C13—C14	1.526 (2)
N3—N4	1.340 (2)	C14—H14A	0.9900
C3—H3	0.9500	C14—H14B	0.9900
C3—C4	1.381 (3)	C14—C15	1.517 (3)
N4—C11	1.346 (2)	C15—H15A	0.9900
N4—C12	1.462 (2)	C15—H15B	0.9900
C4—H4	0.9500	C16—C17	1.493 (3)
C4—C5	1.389 (3)	C17—H17A	0.9800
O4—C16	1.204 (3)	C17—H17B	0.9800
C5—H5	0.9500	C17—H17C	0.9800
C5—C6	1.387 (2)		

C2—C1—N1	127.42 (15)	N2—C10—C9	121.71 (14)
C2—C1—C6	121.84 (15)	N2—C10—C11	108.05 (15)
C6—C1—N1	110.73 (13)	C11—C10—C9	130.23 (15)
C1—N1—C9	124.78 (14)	N4—C11—C10	104.91 (14)
C8—N1—C1	111.05 (13)	N4—C11—H11	127.5
C8—N1—C9	123.92 (14)	C10—C11—H11	127.5
N3—N2—C10	109.17 (14)	N4—C12—H12A	109.2
C1—C2—H2	121.7	N4—C12—H12B	109.2
C1—C2—C3	116.69 (16)	N4—C12—C13	112.12 (14)
C3—C2—H2	121.7	H12A—C12—H12B	107.9
C16—O3—C15	115.84 (17)	C13—C12—H12A	109.2
N2—N3—N4	107.01 (14)	C13—C12—H12B	109.2
C2—C3—H3	119.1	C12—C13—H13A	109.5
C4—C3—C2	121.86 (16)	C12—C13—H13B	109.5
C4—C3—H3	119.1	C12—C13—C14	110.68 (15)
N3—N4—C11	110.85 (14)	H13A—C13—H13B	108.1
N3—N4—C12	120.49 (15)	C14—C13—H13A	109.5
C11—N4—C12	128.65 (15)	C14—C13—H13B	109.5
C3—C4—H4	119.5	C13—C14—H14A	109.5
C3—C4—C5	120.94 (16)	C13—C14—H14B	109.5
C5—C4—H4	119.5	H14A—C14—H14B	108.1
C4—C5—H5	121.0	C15—C14—C13	110.55 (16)
C6—C5—C4	117.91 (17)	C15—C14—H14A	109.5
C6—C5—H5	121.0	C15—C14—H14B	109.5
C1—C6—C7	107.76 (14)	O3—C15—C14	111.78 (17)
C5—C6—C1	120.76 (15)	O3—C15—H15A	109.3
C5—C6—C7	131.49 (16)	O3—C15—H15B	109.3
O1—C7—C6	131.43 (16)	C14—C15—H15A	109.3
O1—C7—C8	123.99 (15)	C14—C15—H15B	109.3
C6—C7—C8	104.58 (13)	H15A—C15—H15B	107.9
N1—C8—C7	105.85 (13)	O3—C16—C17	112.35 (19)
O2—C8—N1	126.76 (16)	O4—C16—O3	122.8 (2)
O2—C8—C7	127.39 (16)	O4—C16—C17	124.8 (2)
N1—C9—H9A	109.0	C16—C17—H17A	109.5
N1—C9—H9B	109.0	C16—C17—H17B	109.5
N1—C9—C10	112.76 (13)	C16—C17—H17C	109.5

H9A—C9—H9B	107.8	H17A—C17—H17B	109.5
C10—C9—H9A	109.0	H17A—C17—H17C	109.5
C10—C9—H9B	109.0	H17B—C17—H17C	109.5

C1—N1—C8—O2	−177.98 (15)	N3—N4—C12—C13	−102.89 (19)
C1—N1—C8—C7	1.98 (16)	C3—C4—C5—C6	−0.3 (2)
C1—N1—C9—C10	75.91 (19)	N4—C12—C13—C14	−174.10 (15)
C1—C2—C3—C4	−0.4 (2)	C4—C5—C6—C1	−0.4 (2)
C1—C6—C7—O1	−178.45 (17)	C4—C5—C6—C7	179.38 (16)
C1—C6—C7—C8	1.13 (16)	C5—C6—C7—O1	1.7 (3)
O1—C7—C8—N1	177.72 (15)	C5—C6—C7—C8	−178.69 (16)
O1—C7—C8—O2	−2.3 (3)	C6—C1—N1—C8	−1.35 (18)
N1—C1—C2—C3	−179.27 (15)	C6—C1—N1—C9	173.01 (13)
N1—C1—C6—C5	179.85 (13)	C6—C1—C2—C3	−0.3 (2)
N1—C1—C6—C7	0.00 (17)	C6—C7—C8—N1	−1.91 (16)
N1—C9—C10—N2	−124.59 (17)	C6—C7—C8—O2	178.06 (16)
N1—C9—C10—C11	55.1 (2)	C8—N1—C9—C10	−110.43 (17)
N2—N3—N4—C11	0.15 (19)	C9—N1—C8—O2	7.6 (3)
N2—N3—N4—C12	179.97 (14)	C9—N1—C8—C7	−172.43 (13)
N2—C10—C11—N4	−0.13 (18)	C9—C10—C11—N4	−179.89 (15)
C2—C1—N1—C8	177.70 (15)	C10—N2—N3—N4	−0.23 (19)
C2—C1—N1—C9	−7.9 (2)	C11—N4—C12—C13	76.9 (2)
C2—C1—C6—C5	0.7 (2)	C12—N4—C11—C10	−179.81 (15)
C2—C1—C6—C7	−179.11 (14)	C12—C13—C14—C15	170.55 (16)
C2—C3—C4—C5	0.7 (3)	C13—C14—C15—O3	−169.84 (16)
N3—N2—C10—C9	−179.99 (14)	C15—O3—C16—O4	1.0 (3)
N3—N2—C10—C11	0.23 (19)	C15—O3—C16—C17	−179.57 (17)
N3—N4—C11—C10	−0.01 (19)	C16—O3—C15—C14	−82.3 (2)

Hydrogen-bond geometry (Å, º)

Cg2 is the centroid of the N2–N4/C10/C11 ring.

D—H···*A*	*D*—H	H···*A*	*D*···*A*	*D*—H···*A*
C3—H3···O2^{i}	0.95	2.50	3.291 (2)	141
C9—H9*B*···*Cg*2^{ii}	0.99	2.67	3.6005 (17)	162

Symmetry codes: (i) *x*−1, *y*+1, *z*; (ii) *x*+1, *y*, *z*.